

Effect of Mn^{2+} -doping on the performance of quantum dots sensitized solar cells

RENBAO WANG^{a,b}, SHAORUI WANG^a, HAIHONG NIU^c, SHIDING MIAO^a, LEI WAN^a, JINZHANG XU^{a,*}

^a*School of Electrical Engineering and Automation, Hefei University of Technology, Hefei 230009, P. R. China*

^b*School of Electrical and Information Engineering, Anhui University of Science and Technology, Huainan 232001, P. R. China*

^c*School of Nuclear Science and Technology, Lanzhou University, Lanzhou 730000, P. R. China*

Mn^{2+} -doped CdS is employed to improve quantum dots sensitized solar cells (QDSSCs) performance. The effects of Mn^{2+} -doping on the performance of QDSSCs are investigated. QDSSCs that are fabricated with Mn^{2+} -doped-CdS/CdSe deposited on mesoporous TiO_2 -nano- SiO_2 hybrid film as photoanode have higher power conversion efficiency under the illumination of one sun (AM1.5, $100\text{mW}/\text{cm}^2$), and exhibit higher activity especially in the short circuit current density (J_{sc}) as compared to the undoped QDSSCs. It is found that certain amount of Mn^{2+} doped in CdS is crucial to make photoelectrons to be trapped and protect them from charge recombination with oxidized polysulfide and/or holes. The 60mM Mn^{2+} -doped concentration is optimal to obtain the highest conversion efficiency (2.45%) in the experiment. The introduced Mn^{2+} as mid-gap states gives a significant enhancement in the performance of corresponding QDSSCs in terms of photocurrent density and power conversion efficiency.

(Received March 4, 2013; accepted January 22, 2014)

Keywords: Mn^{2+} -doped, Quantum dots, Solar cells

1. Introduction

Quantum dots sensitized solar cells (QDSSCs) have drawn much attention due to the extraordinary optical and electrical properties of QDs [1-4]. The unique band character [5, 6], high absorption coefficient [7], and impact ionization effects [8, 9] make them attractive candidates for QDSSCs. QDSSCs are similar to dye sensitized solar cells (DSSCs), and the theoretical maximum power conversion efficiency of QDSSCs is higher than that of DSSCs [10-12]. But up to now, the power conversion efficiency still remains far from satisfactory. The charge recombination at the semiconductor interface is a major limiting factor in obtaining higher efficiency of QDSSCs [13]. To solve the problem, it is feasible to modify the optical and electrical properties of QDs by doping optically active transition metal ions [14-18]. The electronic states in the mid-gap region of QDs can be created, and can alter the dynamics of charge separation and recombination through the dopant. In addition, it is possible to tune the optical and electrical properties of QDs based on the type and concentration of dopant [19]. Synthesis of Mn^{2+} -doped II-VI QDs and their properties have been studied in recent reports [20-22], and Mn^{2+} -doped CdS QDs are already utilized to boost the efficiency of QDSSCs [19].

Our earlier effort to design the TiO_2 -nano- SiO_2 hybrid

film has already resulted in great enhancement in retarding the charge recombination [23, 24]. In the paper, the concentration of Mn^{2+} -doped was studied in the aim of achieving a higher performance of QDSSCs on the basis of the TiO_2 -nano- SiO_2 hybrid film. In order to realize a high coverage of the TiO_2 -nano- SiO_2 hybrid surface and get a good control of the QDs size distribution, Mn^{2+} -CdS and CdSe QDs were assembled onto the TiO_2 -nano- SiO_2 hybrid film by the successive ionic layer adsorption and reaction (SILAR) and the self-assembled monolayer (SAM) respectively. The photoelectrical characterizations have been researched by the current density vs. voltage (J-V) profile and the incident photon to current conversion efficiency (IPCE) spectrum. It reveals that the Mn^{2+} -doped QDSSCs exhibit higher activity especially in J_{sc} as compared to the undoped QDSSCs. The maximum energy conversion efficiency of 2.45% is achieved with Mn^{2+} -doped photoanode. However, higher concentration of Mn^{2+} -doped does not improve the efficiency. The charge recombination is the major factor that limits the power conversion efficiency in QDSSCs. The process of charge injection from excited QDs into TiO_2 is ultrafast and occurs within few picoseconds [25]. The introduction of Mn^{2+} is feasible to modify the photo-physical and electronic characteristics of QDs [15, 16]. The mechanism of Mn^{2+} -doped is to set up electronic states in the mid-gap region of QDs, thus can alter the dynamics of charge

separation and recombination. Mn^{2+} -doped as the mid-gap state makes photoelectrons be trapped and protected from recombination with redox couple and/or holes at the semiconductor interface. Higher concentration of Mn^{2+} can influence the optical and electronic characteristics of QDs, and is disadvantage of co-adsorption of Mn^{2+} and Cd^{2+} ions, which is not facilitated incorporation of Mn^{2+} in the CdS. A conclusion is drawn that the use of Mn^{2+} -doped can enhance the photovoltaic performance of QDSSCs greatly.

2. Experimental

2.1. Materials

TiO_2 powder (~30nm, P₂₅, Degussa), SiO_2 powder (~12nm, Degussa), fluorine-doped tin oxide (FTO, 20V/A) glasses, and Titanium (IV) tetrachloride (TiCl_4 , 99.0%, Beijing Chemical Co.) were used as received to prepare TiO_2 -nano- SiO_2 films. Cadmium oxide (CdO, Aldrich), trioctylphosphine oxide (TOPO, Aldrich), tetradecylphosphonic acid (TDPA, Aldrich), trioctylphosphine (TOP, Aldrich), and selenium (Se, Aldrich) were used to prepare CdSe QDs. Mercaptopropionic acid (MPA, Aldrich) tent to increase CdSe QDs adsorption. The electrolyte was composed of Na_2S (Beijing Chemical Co.), S (Beijing Chemical Co.), and KCl (Beijing Chemical Co.).

2.2. Synthesis of CdSe QDs

CdSe QDs were prepared by the procedure reported in the literature with few modifications [26]. CdO(50mg), TOPO(2000mg), TDPA(280mg), and DDA(900mg) were degassed at 130 °C for 70min, then heat to 305 °C to completely dissolve the precursors under nitrogen. TOPSe (16mg of Se dissolved in 4.0mL of TOP) was quickly injected into the reaction vessel to initiate the reaction. After 3min of growth at 280 °C, the resulting solution was cooled to room temperature. CdSe QDs were precipitated with isopropanol, methanol and toluene, and dissolved in toluene for use. The purification process was repeated three times.

2.3. Ligand exchange of CdSe QDs

MPA (0.2g) was dissolved in methanol (10ml), and its pH value was adjusted to be 11~13 with a saturated solution of NaOH/methanol (0.5M). Certain amount of TDPA-coated CdSe QDs (e.g., 10 mL CdSe QDs in toluene where the optical density is 1.2 unit at wavelength of 545nm.) was mixed with the aforesaid solution ($v/v=1$). The mixed solution was stirred for 30min and centrifuged for 15min [27]. Then, CdSe QDs were precipitated, and dispersed in methanol (10ml). The ligand-exchanged process was repeated three times. The resulting

precipitated was transferred into water for use. Such, CdSe QDs underwent ligand exchange with MPA.

2.4. Fabrication of Mn^{2+} -d-CdS/CdSe-QDSSCs films

The cleaned FTO glasses were immersed into a TiCl_4 aqueous solution (40mM) at 70 °C for 30min. The FTO substrates were coated by the $\text{TiO}_2/\text{SiO}_2$ composite paste via the screen-printing method. Then, the TiO_2 -nano- SiO_2 film was obtained after annealed at 500 °C for 50 min [28]. SILAR was used to assemble Mn^{2+} -CdS onto the TiO_2 -nano- SiO_2 film [29]. To incorporate different Mn^{2+} concentration, three concentrations of manganese acetate (30mM, 60mM, 90mM) were mixed with cadmium nitrate (100mM) respectively. A TiO_2 -nano- SiO_2 film was dipped into a $\text{Cd}(\text{NO}_3)_2$ solution in 1:1 methanol and water for 2min, and rinsed with 1:1 methanol and water, then dipped for another 2min into a Na_2S solution (100mM) in 1:1 methanol and water, and rinsed with 1:1 methanol and water. The incorporated amount of Mn^{2+} -CdS can be increased by repeating the process. The prepared hybrid photoanodes were named as x - Mn^{2+} -d-CdS where x represented the molar concentration of manganese acetate ($x=0\text{mM}$, 30mM, 60mM, 90mM). MPA-coated CdSe QDs was fabricated using the spin-coating method. The spin-coating steps were at 2,500 r.p.m. Each iteration consisted of two steps: (1) three drops of CdSe aqueous solution was dropped onto a static TiO_2 -nano- SiO_2 substrate and spun for 20s; (2) the film was washed by water flush, and spun (~5s) to dry the film. The process was repeated ~5 times to obtain a smooth, shiny CdSe QDs onto the TiO_2 -nano- SiO_2 film. Finally the photoanodes were covered with a layer of ZnS by dipping into $\text{Zn}(\text{NO}_3)_2$ (100mM) and Na_2S (100mM) solutions alternately [30]. Pt-counter electrodes were prepared by screen-printing technique. The two electrodes were sandwiched by thermal adhesive film (Surlyn1702, Dupont). The electrolyte solution consisted of Na_2S (500mM), S (800mM), and KCl (200mM) [31], and was filled through the hole made on the counter electrode [32]. J-V measurement was done with a Keithley model 2440 Source Meter and a Newport solar simulator system at one sun (AM 1.5, 100mW/cm²). IPCE plotted as a function of wavelength was preformed with a QTest station 1000 ADI system (Crowntech Inc.) conducted with a 300W xenon lamp.

3. Results and discussion

3.1 The optical characterization of CdSe QDs

In Fig. 1 (A), CdSe QDs exhibit typical absorption and photoluminescence (PL) properties (a first sharp absorption peak at 545nm, and a band-edge emission with a maximum at 558nm), which reveals that the sizes of

nanocrystals are close to monodisperse. Based on the empirical equations proposed by Yu et al., it is possible to estimate that the mean size of CdSe QDs is to be ~3.0nm [33, 34]. The high crystallinity of CdSe QDs is confirmed by the powder X-ray diffraction (XRD) showed in Fig. 1(B). At high temperatures, CdSe QDs grow in the wurtzite (hexagonal) structure. The diffraction peaks in XRD pattern are assigned to the hexagonal structure of CdSe (JCPDS No.08-0459). Fig. 1(C) shows the

transmission electron microscopy (TEM) image of CdSe QDs. Clearly, TEM image indicates that sizes of these nanocrystals have almost uniform distribution. This result is further verified by high-resolution TEM measurements. The lattice fringes (Fig. 1(D)) extend completely across each nanocrystal, indicating epitaxial growth directly [35]. Such, the method provides us the high-quality and nearly monodisperse semiconductor CdSe nanocrystals.

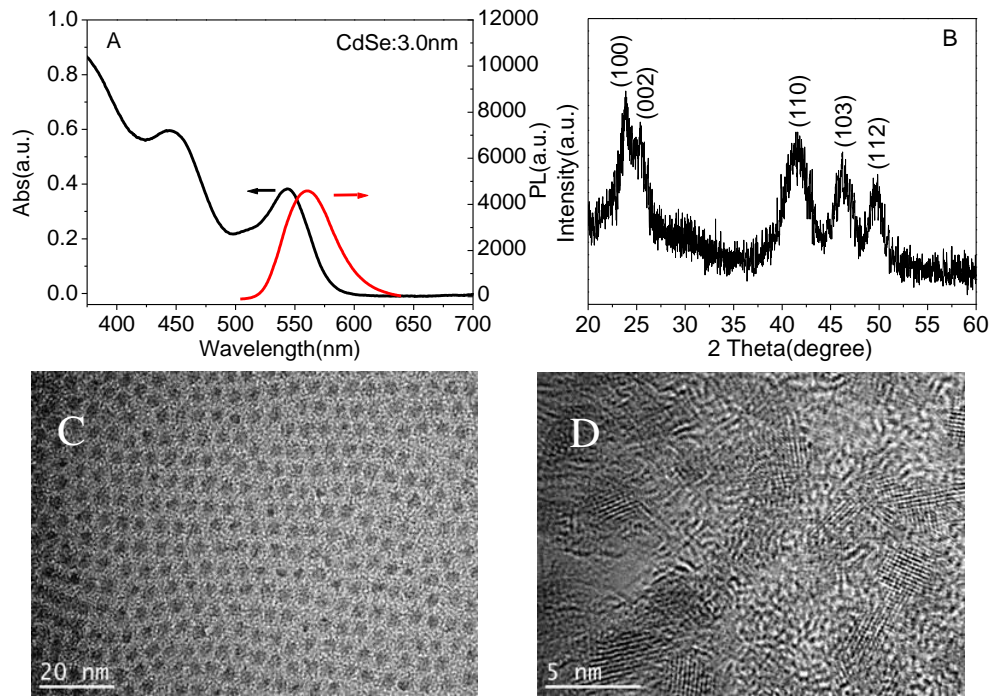


Fig. 1. Absorption and emission spectra (A), XRD pattern (B), TEM image (C), and HR-TEM image (D) of CdSe nanocrystals. The excitation wavelength is 365nm.

3.2 Influence of ligand type

To deposit the prepared CdSe QDs onto the TiO₂-nano-SiO₂ substrate, the TDPA-capped CdSe QDs are transferred into aqueous solution by ligand exchange. In the experiment, mercaptopropionic acid (MPA), which has the short alkyl chain and the hydrophilic group, is utilized to replace the long chain TDPA. Fig. 2 shows the

absorption and PL spectra of CdSe QDs after MPA exchange. It is seen that the absorption peak has a slight shift after ligand exchange. The position of PL peak does not change greatly, but the PL peak of MPA-capped CdSe QDs declines. It suggests that the size of CdSe QDs does not change distinctly, but the passivation effect of MPA becomes weaker than that of TDPA.

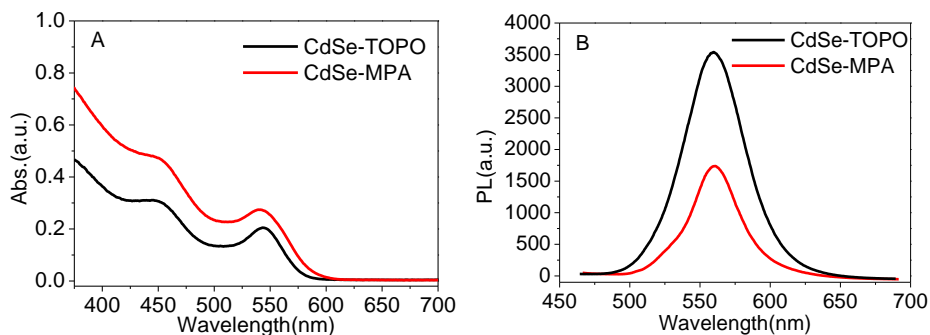


Fig. 2. Absorption (A) and PL spectra (B) of the CdSe QDs after ligand exchange with MPA. The excitation wavelength is 365nm.

3.3. Characterization of Mn^{2+} -d-CdS/CdSe-QDSSCs films

The presence of these materials on the TiO_2 -nano- SiO_2 film can be identified by the atomic force microscopy (AFM) images shown in Fig. 3. Comparing between morphologies of TiO_2 -nano- SiO_2 films with and without QDs, the morphology of the TiO_2 -nano- SiO_2 film becomes rougher (Fig. 3B) after assembling of QDs. The co-sensitization effect of Mn^{2+} -d-CdS and CdSe can clearly be observed by the UV-vis absorbance spectra

shown in Fig. 4. The electrodes have the wider absorption ranges in the visible region below 610nm. In the short wavelength region where both CdS and CdSe are photoactive, the absorbance can be attributed to the co-absorption of the two materials to light. In the long wavelength region, the absorbance can be attributed to CdSe QDs. And all the spectra show that the absorption peaks of electrodes are located at the wavelength of about 545nm corresponding to the first excitonic absorption peak of CdSe QDs.

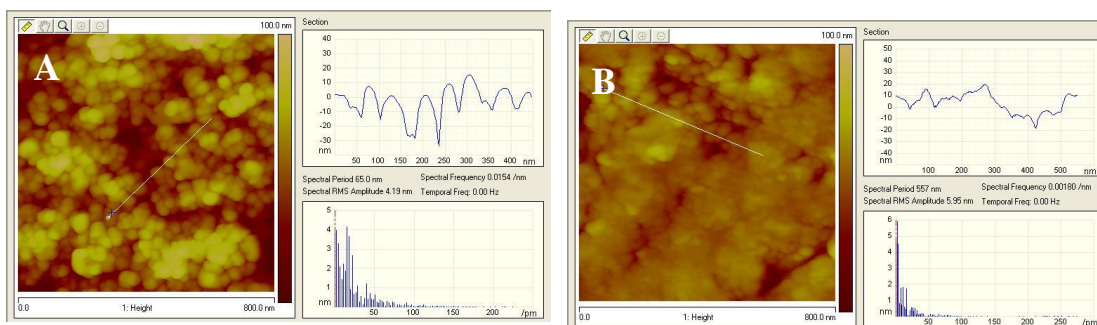


Fig. 3. AFM images of a TiO_2 -nano- SiO_2 film (A) and a film after introduction of Mn^{2+} -CdS using 6 cycles (B).

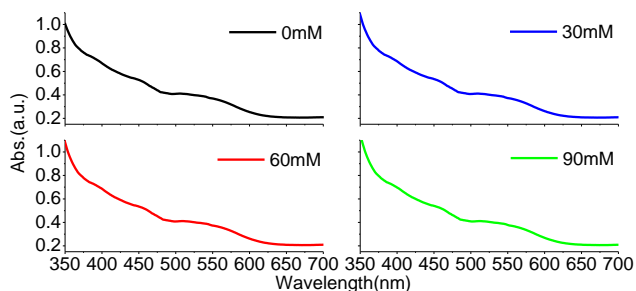


Fig. 4. UV-vis absorption spectra of TiO_2 -nano- SiO_2 films sensitized by Mn^{2+} -d-CdS and CdSe QDs.

3.4 Mn^{2+} -d-CdS/CdSe QDs co-sensitized solar cells

The J-V characteristics of QDSSCs sensitized by Mn^{2+} -d-CdS/CdSe are measured under the illumination of one sun (AM1.5, $100mW/cm^2$). Fig.5(A) shows J-V profiles of the fabricated solar cells. J_{sc} , open circuit potential (V_{oc}), fill factor (FF), and power conversion efficiency (η) are summarized in Table 1.

Table 1. Parameters obtained from the J-V profiles of QDSSCs using various photoanodes.

Sample	Voc(V)	Jsc(mA/cm ²)	FF	η (%)
CdS/CdSe	0.56	8.96	0.37	1.86
30- Mn^{2+} -d-CdS/CdSe	0.57	9.57	0.38	2.07
60- Mn^{2+} -d-CdS/CdSe	0.58	11.75	0.36	2.45
90- Mn^{2+} -d-CdS/CdSe	0.58	10.31	0.39	2.33

It can be seen that the efficiencies of cells get enhanced when the Mn^{2+} concentration ranged from 0mM to 60mM. The power conversion efficiency was 1.86% for

the photoanode without dopants. In particular, the maximum power conversion efficiency of 2.45% is achieved with 60- Mn^{2+} -d-CdS/CdSe co-sensitized solar

cells, and the corresponding J_{sc} is 11.75 mA/cm², V_{oc} is 0.58 V, and FF is 0.36. It is evident that the efficiency and current density have significant increase by employing Mn²⁺-doped. The V_{oc} for CdS/CdSe is 0.56 V, and an increase in the voltage is seen in the Mn²⁺-doped films. The maximum photocurrent (11.75 mA/cm²) exhibits significant increase (30%) in 60-Mn²⁺-d-CdS/CdSe as compared to the corresponding films without dopants (8.96 mA/cm²). The reason is that the mid-gap states created by Mn²⁺-doped make photoelectrons be trapped and protect them from charge recombination with oxidized polysulfide electrolyte and/or holes. The high conversion efficiency highlights the importance of Mn²⁺-doped. The conversion efficiency of QDSSCs is not improved with Mn²⁺-doped photoanode (90-Mn²⁺-d-CdS/CdSe). Higher concentration of Mn²⁺ is disadvantage of co-adsorption of Mn²⁺ and Cd²⁺ ions, which is not facilitated incorporation of Mn²⁺ in the CdS film. The fill factors remain few changes, which implies similar electrochemical limitations

for these QDSSCs.

The IPCE was plotted as a function of wavelength. The IPCE spectra of Mn²⁺-doped CdS/CdSe sensitized solar cells are shown in Fig. 5(B). The spectra match well with the UV-vis light absorption characteristics (Fig. 4), are in good agreement with power conversion efficiency from analysis of J-V profiles too. In the short-wavelength region, it is found the IPCE increases with the increase of concentration ranged from 0mM to 60mM, while it decrease as concentration is 90mM. IPCE values as high as 45% can be achieved for the CdS/CdSe film without dopants. The maximum IPCE values as high as 58% is found at 60-Mn²⁺-d-CdS/CdSe. This result indicates that the mid-gap states created by Mn²⁺-doped are helpful to the injection of an excited electron to TiO₂-nano-SiO₂ film, and excited photoelectrons can be collected by the photoanode efficiently. The long wavelength response of IPCE parallels the behavior seen in the absorption spectra.

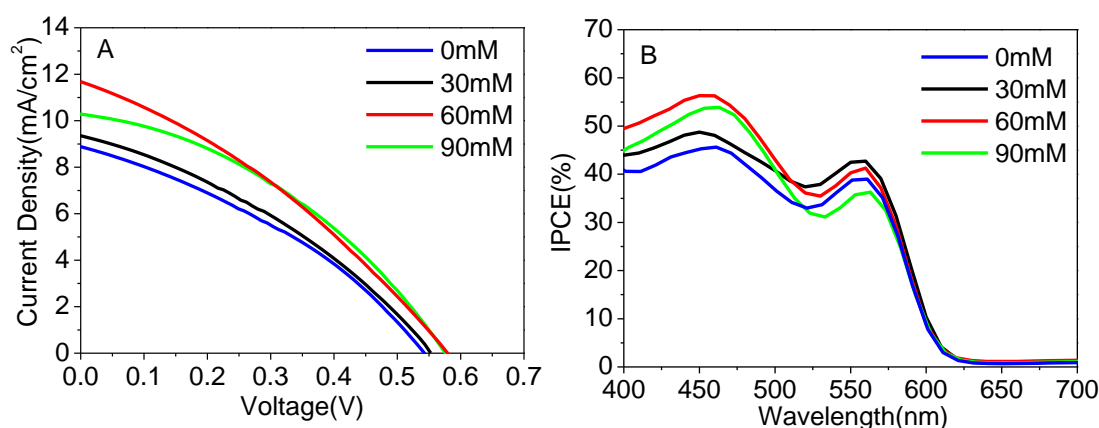


Fig. 5. J-V characteristics (A) and IPCE spectra (B) of QDSSCs using various QDs co-sensitized TiO₂-nano-SiO₂ photoanodes.

4. Conclusion

In summary, we have investigated the influence of Mn²⁺-doped in QDSSCs by studying the photo-conversion properties. Compare to undoped films, the doping films with Mn²⁺ achieve 30% enhancement in power conversion efficiency. The recombination and transport of charge, which influences the J-V and IPCE of QDSSCs, are discussed by comparison with those of the undoped and Mn²⁺-doped photoanodes. It is found that the 60mM Mn²⁺-doped concentration is optimal to obtain the highest power conversion efficiency. The η and IPCE of QDSSCs both decreased with the concentration increased above 60mM. The addition of Mn²⁺ that works as mid-gap states increases the separation of injected electrons and oxidized QDs/redox couple, thereby retards the recombination reactions in QDSSCs.

References

- [1] I. J. Kramer, E. H. Sargent, *ACS Nano*, **5**, 8506 (2011).
- [2] M. M. Byranvand, A. N. Kharat, L. Fatholahi, Z. M. Beiranvand, *J. Optoelectron. Adv. Mater.*, **7**, 961 (2013).
- [3] A. H. Ip, S. M. Thon, S. Hoogland, O. Voznyy, D. Zhitomirsky, R. Debnath, L. Levina, L. R. Rollny, G. H. Carey, A. Fischer, K. W. Kemp, I. J. Kramer, Z. Ning, A. J. Labelle, K. W. Chou, A. Amassian, E. H. Sargent, *Nat. Nanotechnol.*, **7**, 577 (2012).
- [4] P. V. Kamat, *J. Phys. Chem. Lett.*, **4**, 908 (2013).
- [5] M. Grätzel, *Nature*, **414**, 338 (2001).
- [6] A. M. Smith, S. Nie, *Acc. Chem. Res.*, **43**, 190 (2010).
- [7] W. W. Yu, L. H. Qu, W. Z. Guo, X. G. Peng, *Chem. Mater.*, **16**, 560 (2004).
- [8] J. B. Sambur, T. Novet, B. A. Parkinson, *Science*, **330**, 63 (2010).

- [9] V. I. Klimov, *J. Phys. Chem. B*, **110**, 16827 (2006).
- [10] M. C. Hanna, A. J. J. Nozic, *Appl. Phys.*, **100**, 074510 (2006).
- [11] G. J. Meyer, *Inorg. Chem.*, **44**, 6852 (2005).
- [12] X. T. Sui, T. Zeng, G. C. Yin, H. Cheng, X. J. Zhao, *Optoelectron. Adv. Mater.*, **5**, 220 (2011).
- [13] V. Chakrapani, D. Baker, P. V. Kamat, *J. Am. Chem. Soc.*, **133**, 9607 (2011).
- [14] R. N. Bhargava, D. Gallagher, X. Hong, A. Nurmikko, *Phys. Rev. Lett.*, **72**, 416 (1994).
- [15] S. Jana, B. B. Srivastava, N. Pradhan, *J. Phys. Chem. Lett.*, **2**, 1747 (2011).
- [16] R. Beaulac, P. I. Archer, S. T. Ochsenein, D. R. Gamelin, *Adv. Funct. Mater.*, **18**, 3873 (2008).
- [17] R. Beaulac, P. I. Archer, D. R. Gamelin, *J. Solid State Chem.*, **181**, 1582 (2008).
- [18] R. Zeng, M. Rutherford, R. Xie, B. Zou, X. Peng, *Chem. Mater.*, **22**, 2107 (2010).
- [19] P. K. Santra, P. V. Kamat, *J. Am. Chem. Soc.*, **134**, 2508 (2012).
- [20] D. J. Norris, A. L. Efros, S. C. Erwin, *Science*, **319**, 1776 (2008).
- [21] N. S. Karan, D. D. Sarma, R. M. Kadam, N. Pradhan, *J. Phys. Chem. Lett.*, **1**, 2863 (2010).
- [22] A. Nag, R. Cherian, P. Mahadevan, A. V. Gopal, H. A. azarika, A. Mohan, A. S. Vengurlekar, D. D. Sarma, *J. Phys. Chem. C*, **114**, 18323 (2010).
- [23] L. Liu, H. H. Niu, S. W. Zhang, L. Wan, S. D. Miao, J. Z. Xu, *Appl. Surf. Sci.*, **261**, 8 (2012).
- [24] H. H. Niu, L. Liu, H. P. Wang, S. W. Zhang, Q. Ma, X. L. Mao, L. Wan, S. D. Miao, J. Z. Xu, *Acta.*, **81**, 246 (2012).
- [25] K. Tvrđy, P. Frantszov, P. V. Kamat, *Proc. Natl. Acad. Sci. U.S.A.*, **108**, 29 (2011).
- [26] Z. A. Peng, X. G. Peng, *J. Am. Chem. Soc.*, **123**, 183 (2001).
- [27] H. Z. Pan, K. Cheng, Y. M. Hou, J. L. Hua, X. H. Zhong, *ACS Nano.*, **6**, 3982 (2012).
- [28] S. Ito, P. Chen, P. Comte, M. K. Nazeeruddin, P. Liska, P. Péchy, M. Grätzel, *Prog. Photovolt: Res. Appl.*, **15**, 603 (2007).
- [29] C. H. Chang, Y. L. Lee, *Appl. Phys. Lett.*, **91**, 053503 (2007).
- [30] I. Mora-Sero, S. Gimenez, F. Fabregat-Santiago, R. Gomez, Q. Shen, T. Toyoda, J. Bisquert, *Acc. Chem. Res.*, **42**, 1848 (2009).
- [31] Y. Lee, C. Chang, *J. Power Sources*, **185**, 584 (2008).
- [32] C. Zhang, S. Chen, L. Mo, Y. Huang, H. Tian, L. Hu, Z. Huo, S. Dai, F. Kong, X. Pan, *J. Phys. Chem. C*, **115**, 16418 (2011).
- [33] W. W. Yu, X. G. Peng, *Angew. Chem. Int. Ed.*, **41**, 2368 (2002).
- [34] W. W. Yu, L. Qu, W. Guo, X. G. Peng, *Chem. Mater.*, **15**, 2854 (2003).
- [35] X. G. Peng, M. C. Schlamp, A. V. Kadavanich, A. P. Alivisatos, *J. Am. Chem. Soc.*, **119**, 7019 (1997).

*Corresponding author: xujz@hfut.edu.cn